Are Minor and Trace Elements Useful Indicators of Chemical Weathering Processes and Flow-Routing in Subglacial Hydrological Systems?

ANDREW C. MITCHELL,[1] GILES H. BROWN,[2] AND RON FUGE[3]

ABSTRACT:

In Alpine glacierised catchments, snow- and icemelt are chemically enriched and modified during transit though subglacial hydrological systems by distinct bio-geochemical weathering reactions. The nature and extent of these reactions are dictated by waters source and meltwater routing. This chemical modification of meltwaters has been applied in hydrochemical and hydroglacial studies, based mainly on the determination of dissolved *major* ions. In this study we present seasonal variations in the concentration of *minor and trace* elements in bulk-meltwaters and *in-situ* meltwaters from Haut Glacier d'Arolla, Switzerland, and investigate their utility for solute-provenance and flow-routing studies. On seasonal timescales the dissolved concentration of many minor and trace elements (*e.g.* Sr, Rb, Al, Co) are controlled by hydrological parameters such as water residence time and water-rock ratios. However, Li, Be, Mn, Fe, As and Cd appear to be affected by physico-chemical controls such as sorption, (oxi)hydroxide formation and co-precipitation reactions, rather than water residence time alone. Nevertheless, seasonal changes of dissolved minor and trace element concentration ratios reveal important information about solute sources, the nature of weathering processes, and temporal changes in weathering reactions which are associated with hydrological conditions.

Keywords: minor and trace elements; chemical weathering; meltwater chemistry; solute provenance; subglacial hydrology

INTRODUCTION

Chemical characteristics of glacial meltwaters have been widely used to investigate the configuration and dynamics of subglacial hydrological systems (Brown, 2002), based upon the assumption that the composition of bulk outflow reflects distinct biogeochemical weathering reactions which are indicative of the water source and the hydrological system through which the meltwater flowed (Collins, 1979; Raiswell, 1984; Tranter *et al.*, 1993; Brown *et al.*, 1994a; Brown *et al.*, 1996a; Tranter *et al.*, 2002). The composition of the input waters to the glaciers hydrological system provides the initial boundary condition. Thereafter, catchment geology and the configuration and seasonal evolution of the subglacial drainage system dictates the magnitude

---

[1] Department of Geology, University of Toronto, 22 Russell Street, Toronto. M5S3B1. Canada.

[2] School of Geographical Sciences, University of Bristol, University Road, Bristol. BS81SS. UK

[3] Institute of Geography and Earth Sciences, University of Wales, Aberystwyth. SY233QW. UK

and processes of solute acquisition, by controlling parameters which affect chemical weathering processes (*e.g.* water residence time; sediment availability and reactivity; water-rock ratio [Sharp, 1991; Brown, 2002]). The intimate link between glacier hydrology and the chemical evolution of meltwaters, and the physical inaccessibility of subglacial environments has driven the study and application of meltwater quality variations as a remote-sensing tool for geochemical and hydrological processes operating in glacial environments (Sharp, 1991; Brown, 2002). This chemical 'fingerprinting' (Sharp, 1991) of drainage environments has largely considered dissolved *major* ions (*e.g.* Ca^{2+}, Mg^{2+}, Na^+, K^+ and SO_4^{2-}) (*e.g.* Raiswell, 1984; Tranter *et al.*, 1993; Brown *et al.*, 1994a; Brown *et al.*, 1996a). However, minor and trace elements (*e.g.* Sr, Rb, U, Mn, Zn, Pb, Cr, Co, Cu, Al, Ti, Fe) have received little attention (Brown and Fuge, 1998a,b; Mitchell *et al.*, 2001), despite their potential in solute provenance and hydrological flow-path investigations.

Until recently, a generic chemical weathering model where acid-hydrolysis reactions coupled specific proton sources (CO_2 dissolution or sulphide oxidation) with the weathering specific mineral groups (carbonates or silicates) was applied to meltwaters in transit through subglacial environments (Tranter *et al.*, 1993; Sharp *et al.*, 1995a). However, a reappraisal of hydrochemical data from boreholes drilled to the base of Haut Glacier d'Arolla suggested weathering by the dissolution of CO_2 is limited, and that there is a progression of reactions from (i) carbonate and silicate hydrolysis to (ii) sulphide oxidation, first by dissolved oxygen and then by the microbial catalytic reduction of Fe^{3+}, which drives further carbonate and silicate weathering (Tranter *et al.*, 2002). Lithogenic calcium is the dominant cation in most glacial meltwaters, which is assumed to derive entirely from the dissolution of trace carbonates in chemically-limited weathering regimes (Drever and Hurcomb, 1986; Sharp *et al.*, 1995b; White *et al.*, 2005). Lithogenic sulphate is thought to derive entirely from sulphide oxidation, and Na^+ and K^+ from silicate weathering (Tranter *et al.*, 1993; Sharp *et al.*, 1995a; Brown *et al.*, 1996a; Hodson, *et al.*, 2000; Tranter *et al.*, 2002). The rapidity of carbonate hydrolysis suggests carbonate weathering dominates where water residence times are limited, and therefore occurs predominately in a channellised subglacial drainage system. Conversely the slower weathering kinetics of sulphides and silicates suggests chemical enrichment and modification will more preferentially occur where there is a long intimate contact between subglacial waters and sediments, predominately in the distributed subglacial drainage system (Brown *et al.*, 1996a)(Figure 1).

This study aims to investigate the utility of minor and trace elements as indicators of geochemical processes influencing meltwater chemistry by utilizing seasonal variations in elemental and ionic concentrations in bulk meltwaters and in-situ subglacial meltwaters collected at Haut Glacier d'Arolla. These are coupled with rock digests and laboratory water-rock interaction experiments to investigate the source of minor and trace elements beneath the Haut Glacier d'Arolla, and their potential in studies of environmental chemistry and subglacial flow-routing.
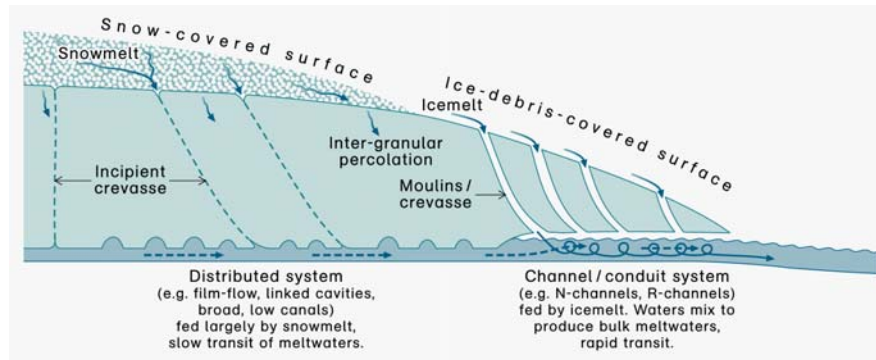

Figure 1. Schematic representation of the subglacial drainage system beneath Alpine glaciers (after Brown, 2002).

FIELD SITE

Haut Glacier d'Arolla (HGA), Valais, Switzerland, is a ~ 4.2 km long temperate glacier which has a maximum ice thickness of ~ 180 m, occupies ~ 6.3 km^2 of a ~ 12 km^2 catchment, and lies on unconsolidated sediments (Sharp *et al*., 1993). Studies of major ion and suspended sediment export suggest chemical denudation constitutes < 1.5% of physical denudation, but is significantly higher than the continental average (Sharp *et al*., 1995a). Dye tracing studies indicate that a hydraulically efficient dendritic channellised subglacial system develops during the meltseason as the seasonal snowcover retreats up-glacier, and glacier-ice ablation and subglacial discharges increase (Nienow *et al*., 1996), concentrating ~ 90% of the annual discharge into the period between May and September. The weathering of suspended sediments within water-filled subglacial channels contributes the majority of Ca^{2+} in bulk meltwaters emerging from the snout of HGA at the height of the ablation season (Brown *et al.,* 1994a; Brown *et al*., 1996b).

The bedrock consists largely of igneous and metamorphic rocks of the Arolla series of the Dente Blanche Nappe (Dal Piaz *et al*., 1977; Mazurek, 1986). The Arolla series comprises mainly Arolla gneisses, hornblende-biotote-tonalites, hornblende-biotite-quartz diorites and gabbros (Tranter *et al*., 1997), and is characterized by weakly metamorphosed Arolla granites and chloritic schist facies. These major units contain trace amounts of geochemically reactive trace minerals such as calcite (up to 0.58%) and pyrite (up to 0.71%) (Tranter, *et al*., 1997). Brown *et al.* (1996b) recorded concentrations of carbonate up to 12% and pyrite up to 5% in the fine fraction (< 5 mm diameter) morainic matrix.

METHODOLOGY

Meltwater sampling

Bulk meltwater and suspended sediment samples were collected twice daily ~ 200 m from the glacier snout in the proglacial channel at 1000 and 1700 h local time (approximating to minimum and maximum diurnal discharge respectively) between 16th June (Calendar Day [CD] 167) and 20th August (CD 232) 1999. Supraglacial meltwaters, snow samples (pre-melt snowpack and fresh snowfall) and rainwater was also collected periodically throughout the study period. Liquid samples were collected in Nalgene LDPE bottles, and snow was collected with a plastic scoop and decanted and melted in zip-lock bags which had been cleaned with the a sub-sample of the snow. *In-situ* subglacial waters were also collected from the base of boreholes drilled to the bed of the glacier during the ablation seasons of 1999 and 2000. The drilling location was chosen on the basis of theoretical reconstruction of the subglacial drainage system, which indicates the occurrence of a major subglacial channel in this area (Sharp *et al.* 1993; Tranter *et al*., 1997; Gordon *et al*., 1998; Hubbard *et al*., 1995). Boreholes were drilled using high pressure hot supraglacial water, supplied from a Kärcher HDS 100BE hot water cleaner, passing through a Conti Asymflex TE DIN rubber hose with a stainless steel tip. Waters were collected from the base of boreholes using a chemically inert sampler, constructed of Plexiglass (after Blake and Clark, 1991). Waters were only collected from boreholes that appeared to be connected to the subglacial hydrological system, as characterized by diurnal oscillations in in-borehole water-level, reflecting diurnal changes in subglacial water pressures (Hubbard *et al*., 1995).

All water and melted snow samples were immediately vacuum filtered through 0.45 μm Whatman cellulose nitrate (WCN) membranes using a Nalgene polysulphone filter unit and hand pump. pH was determined in the field using an Orion 250A portable pH/ISE meter, ROSS combination electrode and automatic temperature compensation probe. Used 0.45 μm WCN membranes and associated suspended particulates were removed from the filter unit with plastic tweezers and retained for suspended sediment concentration (SSC) determination. Bulk discharge was monitored from a rectangular weir located in a hydroelectric power intake structure operated by Grande Dixence SA, located ~ 1.5 km from the glacier snout.

Rock sampling and digests

   A selection of the crushed and milled carbonate minerals from the HGA catchment were totally digested in trace metal grade HCl. In addition, HF total digests were performed on a selection field collected silicate rocks (Table 1).

Water-rock interaction experiments

   In order to evaluate the source of solute during meltwater-subglacial sediment interaction, dissolution experiments were performed on freshly crushed rocks and minerals from the catchment, using boundary conditions approximating to the channellised system at HGA in accordance with methods used by Brown *et al*. (1994a; 1996b, 2002). Samples of the five dominant catchment rock types (quartzite; greenschists; gneiss; schistose granite; meta-gabbro) and carbonates (Table 1) were crushed and milled to produce synthetic suspended particulates. Pyrite was also extracted from greenschists with a stainless steel chisel and was crushed and milled. Scanning electron microscope analysis of true and synthetic suspended particulates indicates that these methods adequately represent the surface morphologies of true suspended particulate loads in glacial environments (Seagren 1999; Brown *et al*., 2001). For each of the five rock types (samples 17 to 22), carbonate (sample 12) and pyrite (sample 22) (Table 1), 4 g of crushed sediment was added to an acid washed 1 litre plastic beaker containing 1 l of air-equilibrated 18 MΩ deionised water and agitated with a polyethylene covered magnetic bar rotated by a magnetic stirrer. These conditions are analogous to near maximum SSCs measured in the field, mixing and reacting in turbulent open subglacial channels with free access to the atmosphere. The apparatus was housed in a refrigerator at a temperature of ∼ 2°C, analogous to the temperature of bulk meltwaters. pH was measured in the beaker as for the field determinations. The reaction mixture was collected at 0, 0.25, 0.5, 1, 2, 4, 8 and 48 hours using acid-washed plastic tubing connected to an acid-washed syringe, and immediately syringe filtered through 0.45 μm WCN membranes.

Major, minor and trace element analysis

   The major ion composition of meltwaters, digest solutions and synthetic meltwaters was determined by ion chromatography (Dionex DX-100). Accuracy was ± 3% and precision ± 5%. Minor and trace element analyses were undertaken by inductively coupled plasma mass spectrometry (ICP-MS) on a VG Elemental Plasmaquad. Accuracy and precision was determined by repeat analysis of standards with concentrations of analytes at concentrations comparable to meltwater samples. Accuracy was ± 15% and precision ± 10% for most analytes (Mitchell *et al*., 2001).

Data presentation.

   To aid interpretation of seasonal data, the 1999 ablation season has been divided into four hydro-climatological periods (prefix P), which are further subdivided into eight sub-periods based upon qualitative analysis of the discharge and meteorological records. The four periods represent major bulk discharge changes during the ablation season. The eight sub-periods are defined as either ablation periods (prefix A) where discharge variations are dominantly driven by solar radiation variations at the glacier surface, or ablation periods affected by significant precipitation events (prefix AP).

Sample	Rock type	Qz	Fsp	APO	Cc	Op/Ox	Oth.
1	Meta-gabbro	-	~45	~55	-	<1	-
2	Diorite	-	70	30	<1	1	-
3	Schistose granite	40	45	-	<1	t	15
4	Graphitic shale	unknown mineralogy					
5	Quartzite	>99	-	<1	t	<1	-
6	Quartzite	>95% quartz, + pyrite + calcite					
7	Diopside marble	1	<1	10	65	2	25
8	Marble	carbonate-rich mineralogy					
9	Pyrite	pure					
10	Calcite vein	>90% calcite					
11	Calcite	pure					
12	Carbonate rock	>90% calcite					
13	Carbonate rock	>90% calcite					
14	Surface carbonate	>90% calcite					
15	Surface carbonate	>90% calcite					
16	Surface carbonate	>90% calcite					
17	Quartzite	>95% quartz, + magnetite					
18	Greenschist	20	-	-	~10	~10	~60
19	Gneiss	-	45	40	-	-	15
20	Schistose granite	40	45	-	t	t	~14
21	Meta-gabbro	-	45	55	-	-	-
22	Pyrite	pure					

RESULTS & DISCUSSION

Meltwater discharge and chemistry

   The composition of snow, supraglacial meltwaters and rain, and output bulk meltwaters from the glacial hydrological system are presented in Table 2, and seasonal plots of selected major ion and minor and trace element concentrations in Figure 3. Snow and supraglacial meltwaters exhibit approximately equal concentrations of major, minor and trace elements. Supraglacial meltwaters comprised of snowmelt in the early ablation season up to the end of P1 and ice-melt once the snow pack had ablated thereafter. However, no significant change in input chemistry was noted, and the highly dilute nature of snow and supraglacial meltwaters suggests much of the elution of chemical species from the snow pack occurred prior to the sampling period. Most significantly, the concentration of major, minor and trace elements in supraglacial meltwaters were significantly modified during transit through the hydroglacial system. Generally, the major ions Mg^{2+}, Ca^{2+}, SO_4^{2-} and HCO_3^- show the greatest enrichment in bulk meltwaters. Sodium, K^+, Cl^-, NO_3^- and minor and trace elements exhibit much lower enrichment factors. Some of the minor and trace elements have enrichment factors ~ 1 or < 1, indicating average concentrations in input waters are broadly similar or less than bulk meltwaters. This is the case for Cr, Mn, Cd, Cs, Hg and Pb.
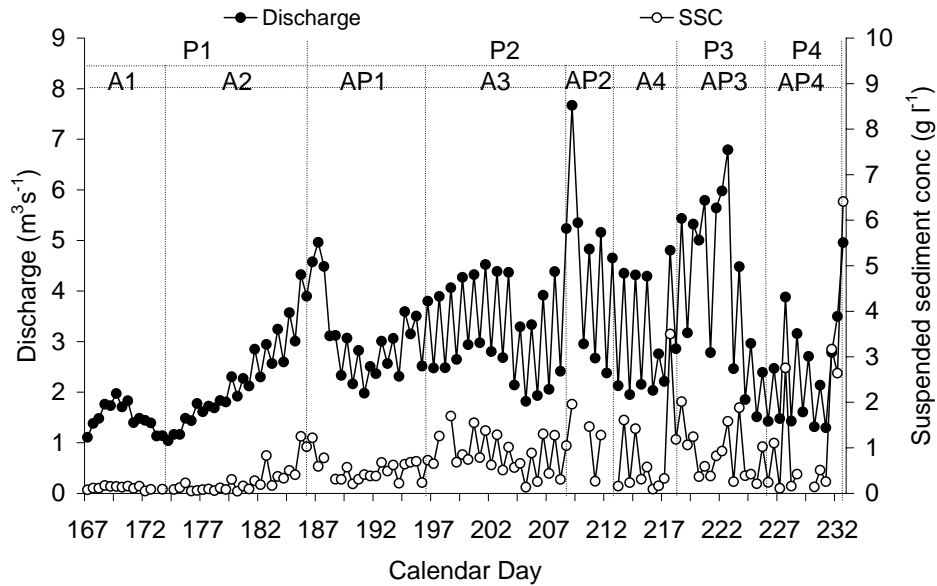
Figure 2. Discharge and suspended sediment concentrations during the 1999 sampling period.

Bulk meltwater concentrations are inversely related to discharge at the seasonal timescale, with high concentrations in P1 and P4, and low concentrations in P2 and P3. Exceptions to this are exhibited by Cl^-, K^+, Ni and U, which are more concentrated during the middle than the early ablation season, and also by Li, Be, Mn, Fe, Co, As and Cd that are more concentrated in the middle than the late ablation season. Bulk meltwater pH was always between 7 and 9 and exhibited a weak positive association with discharge over the ablation season and low seasonal variability in comparison to dissolved solute.

In-situ subglacial meltwaters have been classified by major ion concentrations into three groups, according to the scheme adopted by Tranter *et al.* (1997). Type-2 waters have major ion concentrations similar to bulk meltwaters and are turbid (Table 2), suggesting a subglacial channel-marginal location (Tranter *et al.*, 1997). Type-2 waters exhibit slightly higher minor and trace element concentrations than bulk meltwaters (mean in-situ as % of bulk concentration = 118 %). However U is significantly lower in Type-2 waters than bulk meltwaters. Type-3 waters exhibit major ion concentrations that are on average, 320 % the concentration measured in all bulk meltwaters, and have low SSC's (Table 2), suggesting these waters have had a low water velocity and a long residence time within the distributed system (Tranter *et al.*, 1997). Type-3 waters are also more concentrated with minor and trace elements than bulk meltwaters, but less so than for major ions (in-situ as % of bulk concentration = 240 %). Anomalously, Al, Mo and U are < 80 % less concentrated in Type-3 waters than bulk meltwaters.

Table 2. Concentration ($\mu g\ l^{-1}$) of major, minor and trace elements in snow and input waters to the glacial hydrological system (supraglacial snow- and ice melt, rainwater) and bulk meltwaters during the 1999 ablation season, and in-situ meltwaters at Haut Glacier d'Arolla. Enrichment factors between input waters and bulk meltwater, and the concentration of species in in-situ meltwaters as a percentage of that in bulk meltwater are also shown.

	Supraglacial	Snow	Rain	Bulk Meltwater	Enrichment factors			In-Situ Type 2 (n = 17)			In-Situ Type 3 (n=3)			Type-2 as	Type-3 as
	Median	Median	Median	Median	Supraglacial to Bulk Meltwater	Snow to Bulk Meltwater	Rain to Bulk Meltwater	Minimum	Maximum	Median	Minimum	Maximum	Median	% of bulk meltwater	% of bulk meltwater
Discharge (m^3s^{-1})	-	-	-	2.7	-	-	-	-	-	-	-	-	-	-	-
SSC ($g\ l^{-1}$)	-	-	-	0.41	-	-	-	0.1	1.1	0.5	0.0	0.3	0.1	122	24
pH	7.5	7.7	6.5	8.1	-	-	-	6.7	9.3	8.5	6.7	7.3	7.2	105	89
p(CO_2)	-4.6	-5.13	-3.6	-4.0	-	-	-	-5.2	-2.5	-4.5	-2.9	-2.2	-2.9	112	73
Na^+	34	62	140	370	11	6	3	210	9700	2200	500	970	580	595	157
K^+	36	53	190	370	10	7	2	210	5700	800	250	1100	350	216	95
Mg^{2+}	14	5.6	16	400	29	71	25	180	920	280	540	950	560	70	140
Ca^{2+}	320	140	780	6600	21	47	8	3900	7600	6400	10000	16000	15000	97	227
Cl^-	19	58	140	88	5	2	1	73	18000	2900	730	1200	1200	3295	1364
NO_3^-	25	110	1100	400	16	4	0	0	1200	480	520	1200	770	120	193
SO_4^{2-}	75	1.1	910	5200	69	4727	6	660	6700	4100	5800	17000	9700	79	187
HCO_3^-	1100	470	0	17000	15	36	-	7000	26000	16000	21000	41000	33000	94	194
Li	0.63	0.74	0.70	0.79	1.3	1.1	1.1	0.29	2.0	0.34	1.6	1.9	1.7	43	215
Al	6.6	5.4	6.5	35	5.3	6.5	5.4	12	180	40	11	15	12	114	34
Ti	1.1	1.1	2.0	7.3	6.6	6.6	3.7	7.3	29	10	10	14	13	137	178
Cr	0.87	0.87	1.1	0.93	1.1	1.1	0.8	0.84	3.2	1.5	1.0	1.2	1.0	161	108
Mn	8.8	8.6	11	9.4	1.1	1.1	0.9	8.2	75	11	11	140	14	117	149
Fe	83	74	74	390	4.7	5.3	5.3	370	2400	530	450	4000	560	136	144
Co	0.039	0.057	0.097	0.10	2.6	1.8	1.0	0.14	0.76	0.19	0.23	1.5	0.38	190	380
Ni	0.11	0.07	0.16	0.60	5.5	8.6	3.8	1.1	7.6	1.7	6.5	11	8.5	283	1417
Cu	0.23	0.22	0.80	0.67	2.9	3.0	0.8	1.6	23	4.8	1.6	3.2	2.0	716	299
Zn	1.1	1.1	5.4	6.7	6.1	6.1	1.2	9.0	95	20	24	120	62	299	925
As	0.32	0.26	0.36	0.78	2.4	3.0	2.2	0.27	1.0	0.52	0.83	1.2	1.1	67	141
Rb	0.12	0.18	0.25	0.48	4.0	2.7	1.9	0.50	1.2	0.71	0.49	1.2	0.68	148	142
Sr	0.86	0.41	1.3	15	17.4	36.6	11.5	15	23	19	26	46	46	127	307
Mo	0.75	0.62	0.88	1.6	2.1	2.6	1.8	0.78	1.7	1.3	0.64	0.95	0.85	81	53
Cd	0.18	0.23	0.30	0.21	1.2	0.9	0.7	0.054	0.67	0.23	0.35	0.54	0.40	110	190
I	0.41	0.45	0.75	0.65	1.6	1.4	0.9	1.0	1.6	1.2	1.1	2.1	1.3	185	200
Cs	0.019	0.019	0.028	0.026	1.4	1.4	0.9	0.011	0.28	0.019	0.14	0.24	0.23	73	885
Ba	0.27	0.39	0.41	0.72	2.7	1.8	1.0	0.55	2.5	0.88	2.4	4.0	3.0	122	417
Hg	0.24	0.26	0.20	0.29	1.2	1.1	1.5	0.096	0.43	0.13	0.26	0.41	0.33	45	114
Pb	0.22	0.2	0.4	0.20	0.9	1.0	0.5	0.070	2.9	0.17	0.22	0.42	0.40	85	200
U	0.14	0.11	0.19	0.68	4.9	6.2	3.6	0.069	0.36	0.14	0.087	0.43	0.26	21	38

While the majority of Cl^- and NO_3^- will reflect the release of atmospheric inputs from ice or snow (Sharp *et al*., 1995a; Tranter and Jones, 2000), the enrichment of many minor and trace elements between supraglacial input waters and bulk meltwaters must reflect solute liberation by subglacial chemical weathering processes (Brown and Fuge, 1998a,b; Mitchell *et al*., 2001), as demonstrated for major ions (Brown *et al*., 1994a). The composition of catchment rocks and minerals, and the release of solute from these units will now be investigated to ascertain the lithogenic sources of minor and trace elements, and their utility for investigating temporal changes in weathering reactions which are associated with hydrological conditions.
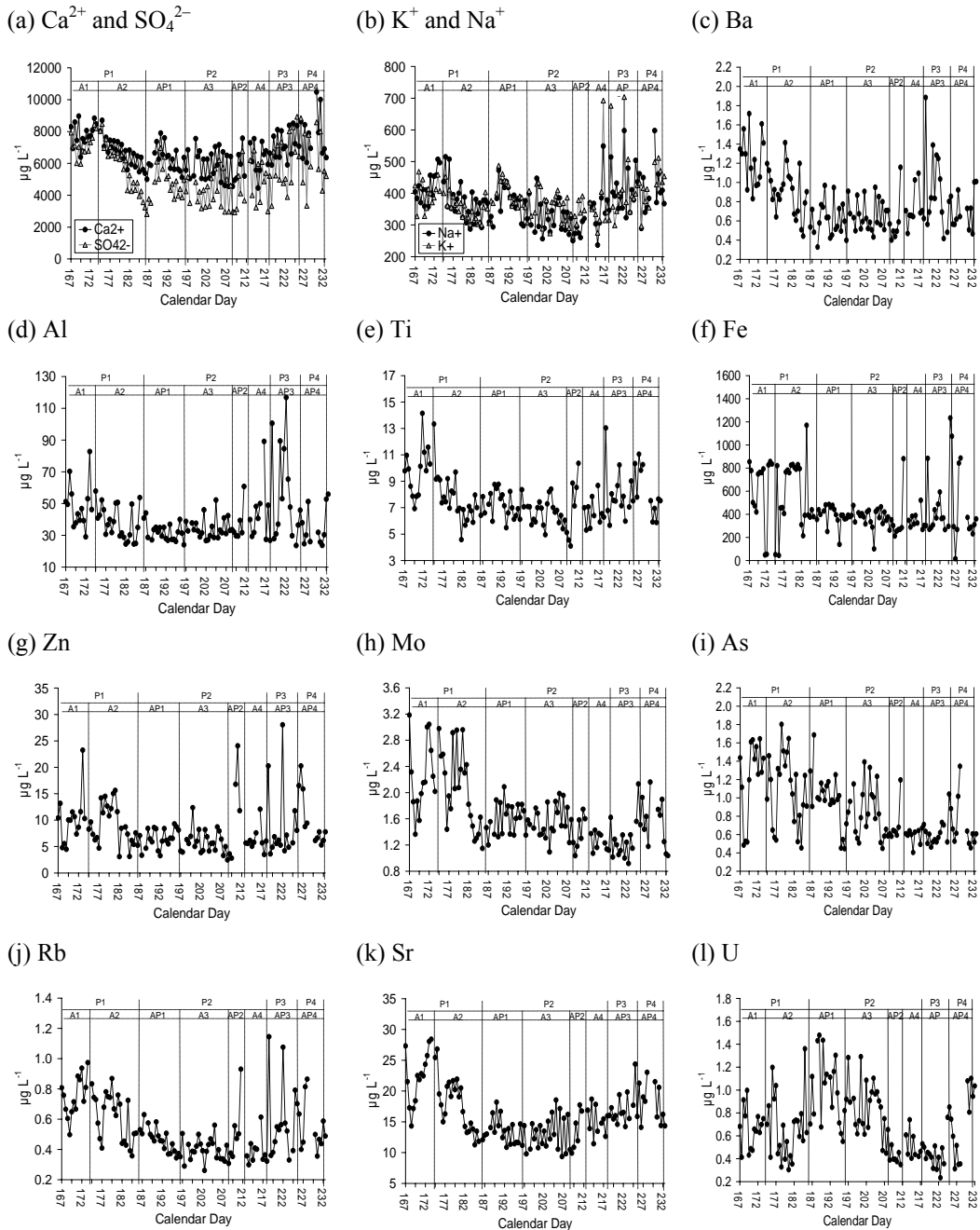
(a) Ca²⁺ and SO₄²⁻

(b) K⁺ and Na⁺

(c) Ba

(d) Al

(e) Ti

(f) Fe

(g) Zn

(h) Mo

(i) As

(j) Rb

(k) Sr

(l) U

Figure 3. Seasonal variations in the dissolved concentration ($\mu g\ l^{-1}$) of selected major ions and minor and trace elements

Rock and Mineral Digests

The elemental composition of major rocks and minerals in the HGA catchment (Table 1) are presented in Table 3. Silicate rocks with a large feldspar and mica content (Samples 1–6) are enriched with Na, K and Mg, relative to marbles, calcite and pyrite. The magnesium content in carbonate minerals is extremely low (< 4 % of the total mass of Ca and Mg) indicating these samples are comprised of $CaCO_3$ (Deer *et al*., 1992). Calcium is relatively abundant in gabbro, graphitic shale, quartz (Sample 6) and less so in schistose granite, diorite and quartz (Sample 5).

56

However marble and calcite samples have significantly higher calcium contents reflecting the purity of calcium carbonate mineralogy in these samples. The high concentration in gabbro is likely to be derived largely from Ca-plagioclase or Ca-clinopyroxene (Tables 1 and 3). Although the mineralogy of the graphitic shale is unknown, the high Ca content is probably detrital carbonate (Levinson, 1980). In quartz and schistose granite, trace carbonate is the only likely source of Ca (Table 3) (Drever and Hurcomb, 1986). These data therefore indicate high concentrations of Ca in non-carbonate and carbonate minerals in igneous and metamorphic rocks.

The average summed mass of minor and trace elements (excluding Sr and Fe) is 2000 mg kg^{-1} in silicate rocks, compared to only 800 mg kg^{-1} in carbonates. Pyrite also exhibits high concentrations of Co, Cu, Zn, Pb and U, as well as Fe, typical of sulphide minerals (Deer *et al.*, 1992). This indicates minor and trace elements are most concentrated in silicate rocks and sulphides, relative to carbonate rocks (Table 3). Carbonate samples (7, 8, 10–16) and silicate rocks which contain trace carbonates (graphitic shale, quartzite) exhibit the highest Sr concentrations. Barium and Mo are present dominantly in silicate rocks compared to carbonates. Carbonates in this catchment are also Fe rich, particularly in secondary carbonates associated with the surface of igneous and metamorphic rocks. Iron is present up to 170000 mg kg^{-1} in Samples 14–16, which is often typical of CaCO$_3$ (Deer *et al.*, 1992).

Table 3. Major, minor and trace element content (mg kg^{-1}) of rocks and minerals from the Haut Glacier d'Arolla catchment from rock and mineral digests. Mineralogical composition shown in Table 1. '–' indicates no calibrated data available. # indicates polyatomic ion interference because of HCl reagent.

Rock / mineral no.	1	2	3	4	5	6	7	8	9	10	11	12	13	14	15	16
Rock / mineral Type	Meta-Gabbro	Diorite	Schistose granite	Graphitic shale	Quartzite	Quartzite	Diopside marble	Marble	Pyrite	Calcite vien	Calcite	Carbonate	Carbonate	Surface carbonate	Surface carbonate	Surface carbonate
Na	14000	23000	32000	890	22000	5000	8000	2700	190	2200	260	75	55	37	120	17
K	22000	39000	23000	40000	50000	4600	12000	9600	0.0000010	690	0.0000010	0	18	0	39	0
Mg	15000	2600	4100	15000	240	2200	7700	5900	53	1000	0.0000010	94	74	210	810	35
Ca	32000	1400	8500	56000	830	61000	210000	200000	910	270000	360000	350000	350000	310000	370000	350000
Fe(AA)	38000	6000	9000	33000	0	3600	16000	16000	260000	3600	0.0000010	-	-	-	-	-
Li	-	-	-	-	-	-	-	-	-	-	-	0.11	0.12	0	0.31	0
Be	-	-	-	-	-	-	-	-	-	-	-	0.040	0.024	0.11	0.16	0.062
Mg	-	-	-	-	-	-	-	-	-	-	-	110	110	280	1100	43
Al	-	-	-	-	-	-	-	-	-	-	-	36	39	35	80	15
Ca	-	-	-	-	-	-	-	-	-	-	-	380000	340000	290000	320000	260000
Sc	16	4.0	5.1	35	0.72	1.6	8.3	9.8	0.13	4.4	2.2	1.8	1.8	1.5	10	1.1
Ti	370	40	74	620	12	46	160	190	3.9	110	78	480	470	380	460	330
Cr	110	7.7	12	200	7.4	11	38	45	5.6	14	7.1	#	#	#	#	#
Mn	-	-	-	-	-	-	-	-	-	-	-	44	42	350	1600	20
Fe	-	-	-	-	-	-	-	-	-	-	-	100000	110000	110000	170000	100000
Co	14	19	14	14	24	18	23	12	0.15	8.0	5.4	3.5	3.5	4.5	2.1	1.3
Ni	66	10	21	120	5.5	18	54	62	34	40	34	22	21	25	26	18
Cu	25	7.4	6.4	40	4.5	11	17	24	300	7.8	3.9	0.26	0.43	2.2	3.1	0.15
Zn	130	42	39	140	18	100	61	63	690	12	3.6	14	12	12	4.2	3.2
Ga	40	20	22	66	13	5.3	18	15	0.56	1.9	1.2	0	0	0.13	0	0
As	15	4.7	11	40	5.3	7.7	35	37	68	36	120	#	#	#	#	#
Rb	120	200	99	190	160	19	60	45	0.0000010	6.1	8.2	8.6	8.0	5.4	4.7	5.2
Sr	810	29	80	1300	17	410	2600	3500	5.8	2500	2900	2900	2900	2000	1600	1900
Mo	1.8	0.95	1.0	0.67	0	0.48	1.7	0.41	0.24	0.27	0.035	0.043	0.18	1.6	0.47	0.26
Cd	0.44	1.1	1.4	0.40	0.22	0.42	1.2	1.4	0.74	0.35	0.29	0	0	0.15	0.72	0
Cs	2.4	2.3	1.5	4.5	1.3	0.30	1.0	0.60	0	0	0	0	0	0.011	0.070	0
Ba	840	250	350	1300	250	130	400	230	2.1	24	2.6	8.4	1.5	19	2.8	6.3
Nd	50	34	38	86	0.32	4.6	20	23	0.39	7.8	0.56	0.031	0.015	0.52	0.27	0.054
Pb	10	4.9	2.4	23	9.7	30	6.2	9.1	1900	5.3	3.8	1.9	1.9	2.1	3.8	2.3
Bi	2.3	0.60	0.70	5.4	0.77	2.1	0.090	0.56	15	1.4	1.1	0.047	0.061	0.074	0.12	0.13
Th	18	21	13	30	2.8	1.4	6.0	6.1	0.51	2.9	0.010	0.0021	0.0032	0.032	0.073	0.0075
U	1.8	3.3	1.7	2.2	0.86	0.21	3.4	3.7	11	0.25	0.010	0	0	0.031	0.012	0

Water-rock interaction experiments

Solute concentrations obtained during chemical weathering are dependent not only on the element content of minerals, but also the relative dissolution rate of the minerals, the position of elements in the mineral lattice, and the mobility of species in solution after release (Stumm and Morgan, 1996). Median solute concentrations obtained from water-rock interaction experiments performed on catchment rocks and minerals (Table 1) are broadly proportional to the element content of the rock or mineral (Figure 4; Table 4). For example K$^+$ is liberated mostly from gneiss, schistose granite and gabbros (median < 2500 µg l^{-1}) which have a high K-feldspar and K-mica content. Quartzite dissolution also liberates K$^+$ at a median concentration of 1300 µg l^{-1} which probably reflects the presence of small amounts of muscovite, biotite and microcline (Table 1). Calcium is liberated to a high concentration by most of the rock samples except quartzite, especially by greenschist, gneiss and calcite, where Ca^{2+} is liberated at median concentration of between 5900 and 8200 µg l^{-1} (Figure 4; Table 4). Sulphate concentrations derived from the freshly crushed sulphide inclusive rocks (Samples 18 and 20) are very low (< 220 µg l^{-1}), and only 5 % of median bulk meltwater concentrations (Table 4). Limited SO$_4^{2-}$ liberation has been noted in previous water-rock interaction experiments using proglacial sediments (Brown *et al.*, 1994a; 1996b) and synthetic suspended sediments (Seagren, 1999). This supports previous assertions that sulphide oxidation is limited in subglacial channels, although this does not appear to reflect

sulphide exhaustion as previously suggested (Brown *et al*., 1994a; 1996b). Rather it may reflect low dissolved oxygen concentrations (low pO_2 conditions in bulk meltwaters draining HGA have been presented by Brown *et al.,* 1994b) or that sulphides are oxidised in anoxic environments by other oxidising agents such as Fe^{3+} (Bottrell and Tranter, 2002; Tranter *et al*., 2002). Indeed, while the SO_4^{2-} concentration derived from pure pyrite dissolution (Sample 22) is very high (median = 68000 μg l^{-1}), this concentration is only ~13 times that of the bulk meltwater (Figure 4; Table 4) indicating that pyrite oxidation is still *relatively* limited in the experiment relative to the high pyrite-water ratio used.

The concentration of minor and trace elements derived from the dissolution of silicate rocks and calcite also reflects general differences in the minor and trace element content of the rock types (Figure 4), although these differences are not as marked as for major ions. Indeed, carbonate (Sample 12) can generate concentrations of elements such as Al, Ti, Zn and As comparable to the dissolution of silicate catchment rocks (Figure 4). This sample has a low concentration of these elements relative to silicates (Table 3) so rapid carbonate dissolution kinetics must account for the high concentrations generated. The experiments also confirm that Mn and Cr are not significantly enriched by chemical weathering under conditions analogous to the subglacial channellised system, as suggested by the lack of solute enrichment between supraglacial and bulk meltwaters (Table 2).

Table 4. Median concentration of major ions, and minor and trace elements (μg l^{-1}) during laboratory experiments between fleshly crushed rock material from the Haut Glacier d'Arolla catchment and deionised water

| Rock / mineral type	Quartzite	Greenschist	Gneiss	Schistose granite	Gabbros	Carbonate rock	Pyrite
Rock / mineral no.	17	18	19	20	21	12	22
pH	8.4	10	10	9.9	8.8	10	8.4
Na^+	43	36	550	550	570	66	91
K^+	1300	190	2500	2000	1600	120	110
Mg^{2+}	49	97	340	190	800	310	37
Ca^{2+}	110	5900	6900	2400	3400	8200	3200
SO_4^{2-}	43	220	0	31	0	51	68000
Li	0.90	0.79	1.1	1.6	2.5	1.1	2.3
Be	0.078	0.094	0.045	0.16	0.083	0.11	0.075
Al	19	33	280	200	100	40	8.4
Sc	0.0084	0.18	0.58	0.85	0.65	0.36	0.70
Ti	0.80	5.5	6.6	4.5	4.9	8.4	53
Cr	0.40	0.33	0.28	0.31	0.54	0.54	1.0
Mn	2.4	2.0	1.1	10	5.7	2.4	63
Fe	180	380	330	200	120	320	1300
Co	2.8	0.36	0.32	0.35	0.32	0.051	5.1
Ni	4.4	5.1	3.6	3.6	2.2	2.9	23
Cu	1.4	0.56	0.75	1.1	1.2	1.0	1.3
Zn	180	21	9.6	9.0	7.5	9.4	22
Ga	0.18	0.15	0.66	0.99	1.1	0.17	1.3
As	0.62	0.55	0.41	0.71	0.43	0.35	0.70
Rb	1.1	0.22	3.5	5.2	3.0	0.70	1.3
Sr	0.35	9.1	3.9	2.1	2.5	470	61
Mo	0.30	0.47	0.49	1.6	1.5	0.31	0.95
Cd	0.28	0.21	0.23	0.58	1.3	0.31	0.51
Cs	0.15	0.13	0.12	0.20	0.20	0.15	0.22
Ba	0.36	0.28	1.9	1.6	1.1	2.3	19
Nd	0.15	0.16	0.13	0.24	0.27	0.13	0.20
Pb	0.28	0.20	0.16	0.47	0.34	0.25	0.58
Bi	0.026	0.020	0.021	0.025	0.024	0.0017	0.037
U	0.021	0.042	0.023	0.028	0.035	0.014	0.036
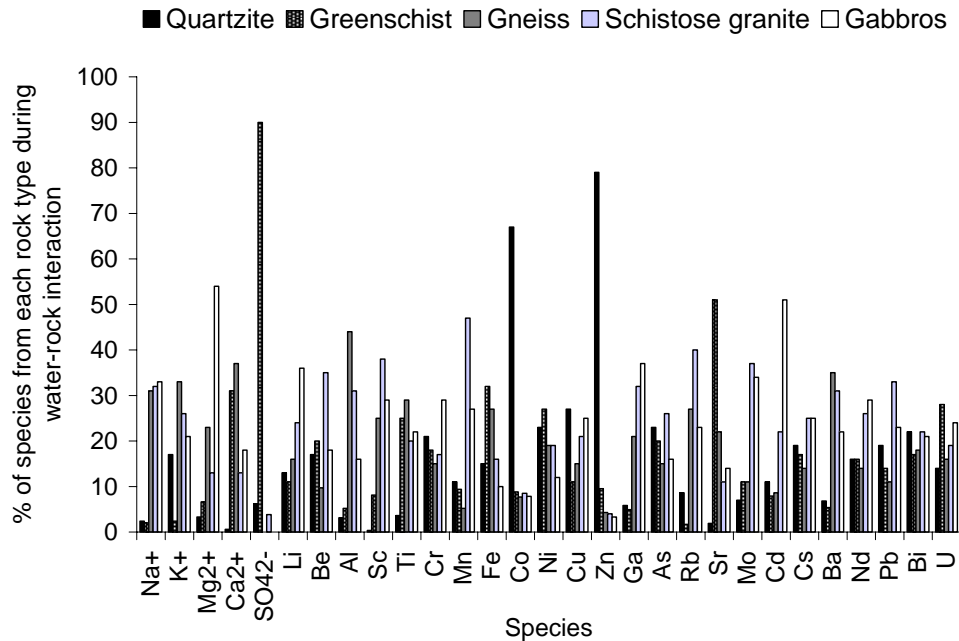
Figure 4. Percentage distribution of the median concentration of major ions and minor and trace elements ($\mu g\ l^{-1}$) generated from different rock types from the Haut Glacier d'Arolla catchment during laboratory experiments between fleshly crushed rock material and deionised water.

Lithogenic sources of major, minor and trace elements.

Table 5 describes the likely provenance of major, minor and trace elements in the subglacial hydrological system beneath HGA, based upon rock digests and water-rock interaction experiments. Trace carbonates have been shown to account for high Ca^{2+} fluxes in igneous bedrock catchments (Drever and Hurcomb, 1986; White *et al*., 2005), and have been assumed to provide all Ca^{2+} in previous subglacial solute provenance studies, even in predominately igneous or metamorphic settings (*cf.* Sharp *et al*., 1995a; Brown *et al*., 1996a). However, these data suggest that high Ca^{2+} concentrations may be derived from the dissolution of carbonates, trace carbonates in igneous rocks and non-carbonate sources beneath HGA. Magnesium release from carbonates is highly preferential relative to its abundance in carbonate minerals. For example the Ca / Mg ratio in carbonate (Sample 12) is 3600 whereas the ratio during solute release from the water-rock interaction experiment is only 27 (Table 6). Conversely Mg^{2+} release from Mg-silicate inclusive rocks (*e.g.* schistose granite, Samples 3 and 20) is retarded relative to Mg abundance in the rock. This suggests Mg in meltwaters at HGA is derived mainly from the preferential release of Mg by incongruent calcite dissolution. Similarly, Sr is derived dominantly from calcite, although Sr release from non-carbonate sources is also apparent. Calcium / Sr ratios in bedrock may be similar between carbonate and non-carbonate rocks (Table 6); however the Ca / Sr ratio from water-rock interaction experiments for calcite and calcite inclusive rocks (Samples 12 and 18; Table 6) are much lower than for apparently calcite free rocks. This indicates that Sr is also preferentially released from carbonates, and is therefore a good minor element indicator of calcite weathering in subglacial environments. Fairchild *et al*. (1994) also noted higher Ca / Sr and Ca / Mg ratios in the carbonate bedrock beneath Glacier de Tsanfleuron than in water-rock interaction experiment solutions, which were similarly attributed to the preferential release of the guest element by incongruent carbonate dissolution. Guest elements are often released preferentially because of the weaker bonds formed during isomorphic replacement (Carroll, 1974).

59

Table 5. Likely dominant sources of minor and trace elements in the subglacial hydrological system at Haut Glacier d'Arolla. Based upon the proportion of elements derived from the dissolution of each rock/mineral type (Figure 5), their mineralogical composition (Table 1), and likely natural geochemical associations in rock-forming minerals (after Rienmann and Caritat, 1998).

Element / species	Likely dominant mineral source	Comments
Na^+	Albite	Dominantly from gneiss, schistose granites and gabbro. All contain plagioclase
K^+	K-silicates	No dominant source. Very low from greenschists.
Mg^{2+}	Carbonates	High concentrations in non-calcite inclusive rocks, but preferentially released by calcite during water rock-interaction
Ca^{2+}	Calcite, Ca-silicates	Dominantly from calcite inclusive rocks, but can be generated by Ca-silicates (plagioclase and pyroxene) at comparable concentrations during water rock-interaction
SO_4^{2-}	Pyrite or gypsum	Low concentrations from all rock types. Highest during water rock-interaction from greenschist (pyrite inclusive) and pyrite dissolution.
Li	Aluminosilicates: Biotite or amphiboles	Highest concentration from granites and gabbros – non carbonate source.
Be	Silicates: Plagioclase or micas	Highest concentration from granites – non carbonate source.
Al	Aluminosilicates	Highest concentration during water rock-interaction from granites and gabbros; which are proportionally dominant in aluminosilicates.
Sc	Aluminosilicates: Pyroxenes, amphiboles, biotite	No dominant source in experiments.
Ti	Aluminosilicates: Micas or sphene. Oxides	No dominant source in experiments.
Cr	Conservative – some from pyroxene	Highest concentration during water rock-interaction from gabbro.
Mn	Conservative – some from silicates (olivine, pyroxene, amphibole, micas). Fe oxides, sulphides.	Highest concentration during water rock-interaction from granites and gabbros; which are proportionally dominant in aluminosilicates. Non-carbonate source. Hard to determine particular silicate source.
Fe	Pyrite, ferromagnesian minerals and calcite	Highest concentration during water rock-interaction from greenschists, although high concentrations derived from other silicates and calcite.
Co	Pyrite, magnetite or ferromagnesian minerals	Highest concentration from quartzite during water rock-interaction.
Ni	Pyrite, micas (chlorite) or ferromagnesian minerals	Highest concentrations from greenschist and quartzite during water rock-interaction.
Cu	Magnetite and pyroxene	Highest concentrations from quartzite and gabbros during water rock-interaction – very different mineralogy suggests different sources.
Zn	Magnetite; maybe some from pyrite or spalerite	Highest in quartzite.
Ga	Feldspars	Highest concentration from granites and gabbros during water rock-interaction; which are proportionally dominant in aluminosilicates. Non-carbonate source.
As	Feldspars, magnetite, pyrite	No dominant source in experiments.
Rb	K-silicates: microcline, biotite, muscovite	Highest concentration from gneiss, granites and gabbros during water rock-interaction. Non-carbonate source.
Sr	Calcite	Highest from greenschist during water rock-interaction. Much less from non-carbonate inclusive rocks.
Y	Biotite, feldspars, pyroxene	No dominant source in experiments.
Mo	Sulphides, apatite.	Highest concentration from granites and gabbros during water rock-interaction.
Cd	Plagioclase or possible biotite	Highest concentration from gabbros, and less so granites during water rock-interaction. Only common minerals are plagioclase, although not suggested in geochemical literature.
Sb	Mg-Olivine	Highest concentration from gabbros during water rock-interaction.
Cs	Micas or K-feldspar	Highest concentration from gneiss, granite and less so gabbros during water rock-interaction. Non-carbonate source.
Ba	Micas or K-feldspar. Baryte.	Highest concentration from granites and gabbros during water rock-interaction. Non-carbonate source.
Nd	Plagioclase	Highest concentration from gabbro during water rock-interaction.
Pb	Plagioclase. Alkali feldspar. Pyrite	Highest in granite and gabbro during water rock-interaction.
Bi	Apatite. Pyrite	Highest in granite and gabbro during water rock-interaction.
U	Apatite, silicates.	Highest from greenschist and gabbro during water rock-interaction.

Iron concentrations derived from the dissolution of pyrite, silicate rocks and carbonates are broadly similar, indicating Fe may be derived from pyrite, ferromagnesian minerals and calcite (Figure 4 and Table 4). However the calcite-water ratio required to generate such Fe concentrations is well in excess of that in subglacial meltwaters beneath HGA, due to the trace sulphide content of the bedrock (Table 1), suggesting Fe derives from both the hydrolysis and acid hydrolysis of ferromagnesian minerals and from pyrite oxidation. Therefore Fe offers limited utility for identifying specific lithogenic sources in subglacial systems at HGA.

Many of the remaining minor and trace elements appear to be useful indicators of lithogenic provenance in subglacial environments. Broadly, Al, Ti, Ba and Rb are indicative of aluminosilicate weathering. For example Rb may be indicative of K-silicate weathering, Ti and Ba of mica weathering. Molybdenum may be indicative of sulphide (MoS_2) or apatite weathering. Indicators of pyrite weathering are less clear because magnetite and ferromagnesian minerals appear to contain and release high concentrations of similar elements, such as Zn, Co and Ni. Lead is present at high concentrations in sulphides (potentially as $PbSO_4$) (Table 3) but no dominant rock or mineral source is obvious for Pb during rock dissolution (Figure 4). While pure calcite dissolution can generate high concentrations of Al, Ti, Zn and As, it is logical to conclude that the concentration of most minor and trace elements will be controlled by silicate dissolution or the oxidation of trace sulphides, because carbonates are proportionally small in catchment bedrock and their minor and trace element concentrations are relatively low.

Controls on minor and trace elements in glacial meltwaters

Bulk Meltwaters. The seasonal inverse dissolved concentration-discharge relationship exhibited by many minor and trace elements in bulk meltwaters, including Al, Ti, Rb, Sr, Mo and Ba (Figure 3), is likely to reflect the seasonal evolution of the subglacial hydrological system, as is apparent from major dissolved ions (Brown *et al.*, 1996a). The relatively high concentrations of many dissolved minor and trace elements early in the ablation season (P1) suggest that these waters may have had a long residence time in the subglacial hydrological system. These may have been stored subglacially over the previous winter and / or have been transported slowly through an inefficient distributed subglacial hydrological system (Nienow *et al.*, 1996). In such environments, water would have had a long and intimate contact with reactive subglacial sediments, allowing significant dissolved minor and trace element acquisition, predominately from silicate dissolution or the oxidation of trace sulphides, as suggested by rock digests and water interaction experiments. Conversely, the lower dissolved concentration of minor and trace elements in meltwaters at the height of the ablation season (P2 and P3) suggests that conditions for solute acquisition are less favourable as the channellised system expands headwards during the ablation season. Part of the concentration decrease will reflect dilution of the concentrated delayed-flow from the distributed system with dilute supraglacial meltwater, but mixing is not conservative since minor and trace elements will liberated from suspended sediments in the channellised system, as demonstrated in water-rock interaction experiments (Figure 4; Table 4; *cf.* Brown *et al.,* 1994a; 1996b). However there will be a mean reduction in water residence and water-rock interaction times in the subglacial environment, which will retard net solute enrichment relative to the early ablation season. The higher dissolved concentrations of minor and trace elements at the end of the ablation season (P4) suggests that, although an efficient channellised system will still exist beneath the glacier, the meltwater generated is not sufficient to generate flow velocities comparable to those at the height of the meltseason (Nienow *et al.*, 1996), and as a result, water-rock interaction times and thus dissolved minor and trace element concentrations will increase.

However, the concentration of minor and trace elements such as Ni and U which are not inversely related to discharge, and Li, Fe and As which do not exhibit an increase in concentration in the late ablation period as discharge decreases (Figure 3), suggests such solutes are affected by physico-chemical controls such as sorption, (oxi)hydroxide formation and co-precipitation reactions, rather than water residence time alone, as has been ascertained from the complexity of solute mobility over time during water rock interaction experiments (Mitchell *et al.*, 2001; Mitchell, 2002). Indeed, it has previously been shown that many minor and trace elements are dominantly transported as labile species on the surface of suspended sediments, sorbed onto sediment or co-precipitated in oxyhydroxides (Mitchell *et al.*, 2001; Poulton and Raiswell, 2005). In the case of Mn, Cs and Cd which exhibit little solute enrichment in the subglacial environment, seasonal concentration variations appear to reflect the simple dilution of supraglacial input meltwaters.

In-situ. The high concentration of major, minor and trace elements in Type-3 waters relative to bulk meltwaters are indicative of long residence times and intimate contact with subglacial sediments, and support the assertions above that significant quantities of minor and trace elements are acquired in the distributed subglacial hydrological system. Low SSCs may also account for the low Al concentration in Type-3 waters, if < 0.45 μm colloidal matter often accounts for a large proportion of measured Al (*e.g.* Bentoit and Rozan, 1999). Type-2 waters have broadly similar concentrations as bulk meltwaters because they are a mixture of delayed-flow and quick-flow waters (*e.g.* Hubbard *et al.*, 1995).

Minor and trace elements as indicators of solute provenance and flow routing

We now consider ratios of elements that are appear to be primarily controlled by hydrological conditions on the seasonal timescale (Sr, Rb, Ba, Al, Ti, Ca^{2+}, Mg^{2+}, K^+ and Na^+) and have been determined to be from the same lithogenic source (intra-mineral) (*e.g.* Fairchild *et al.* 1994; 1999; Jacobson *et al.*, 2002), and contrasting lithogenic sources (inter-mineral) (*cf.* Brown *et al.*, 1996a; Sharp *et al.*, 1995a)**.** We use these to assess the utility of dissolved minor and trace elements for

determining the nature of weathering processes and seasonal changes in solute provenance and flow-routing in the subglacial environment.

Intra-mineral ratios. Carbonates: The Ca / Sr ratios during *in-vitro* dissolution of pure calcite are relatively low (Table 6). Conversely, Ca / Sr ratios derived from the dissolution of other rock types is much greater than in glacial meltwaters due to the limited availability of either trace or mineral carbonates (Table 6). During dissolution experiments using individual rocks/minerals, even greenschists, with a relatively high calcite content, cannot generate as lower Ca / Sr ratio as bulk meltwaters. This could reflect higher calcite abundance in bedrock than in the water-rock interaction experiments, although this seems unlikely since the calcite abundance in the greenschist sample is ~ 10 %. Therefore, this more likely reflects non-carbonate sources (*e.g.* Ca-silicates) of Ca.

K-silicates: The K / Rb ratio in silicate bedrock is much lower than the aqueous ratio during the dissolution of silicate rocks (Table 6), which suggests K is preferentially released over Rb by incongruent K-silicate dissolution. K / Rb ratios in bulk meltwaters are in the range of those from silicate rock dissolution, and are closest to greenschist and gneiss. However, greenschist generates low K and Rb concentrations whereas gneiss provides the highest concentrations from the silicate rocks dissolved, suggesting gneiss may provide the majority of K and Rb in bulk meltwaters relative to other rock types.

Pyrite and magnetite: Cobalt, Zn and to a lesser extent Ni, appear to be derived dominantly from pyrite and magnetite in dissolution experiments (Figure 4). The Zn / Co ratio for quartzite (in which magnetite is present) is exactly the same as bulk meltwaters, whereas the ratio from greenschist (pyrite inclusive) is lower, and extremely low from pure pyrite. This suggests magnetite provides the majority of Zn and Co to meltwaters. However the Ni / Co ratio from pyrite is much closer to bulk meltwater values than the ratio from quartzite dissolution, suggesting a predominantly pyrite origin of these elements to meltwaters (Table 6). Evidently it is hard to identify elements that are derived exclusively from pyrite. These data demonstrate the complexity of using intra-mineral ratios in catchments underlain by complex geology. While mobile minor and trace elements that are predominantly associated with a particular mineral type may be useful for isolating solute sources (*e.g.* Sr), more often the multiple mineral sources and complex physico-chemical behavior (Mitchell *et al*., 2001; Mitchell, 2002) appears to limit their use as lithogenic tracers. Thermodynamic speciation calculations appear to enhance their utility by allowing the solid-solution state of elements to be predicted (Mitchell, 2002; Mitchell *et al*., 2001).

Table 6. Intra-mineral and inter-mineral element ratios from rock digests, water-rock interaction experiments and meltwaters from the 1999 ablation period (CD 167 – 232) at Haut Glacier d'Arolla.

	Ratio	Intra-mineral element ratios							Inter-mineral element ratios								
		Ca / Sr	Ca / Mg	K / Na	K / Rb	Al / Ti	Zn / Co	Ni / Co	Sr / Rb	Sr / Al	Ca / Na	Ca / K	Sr / SO$_4^{2-}$	Ca / SO$_4^{2-}$	Sr / Co	K / SO$_4^{2-}$	Al / Co
Digests																	
Meta-Gabbro	1	39	2.1	1.5	190	-	9.5	4.8	7.0	-	2.2	1.4	-	-	59	-	-
Diorite	2	48	0.54	1.7	200	-	2.2	0.53	0.15	-	0.059	0.036	-	-	1.5	-	-
Metagranite	3	110	2.1	0.71	230	-	2.8	1.5	0.80	-	0.27	0.38	-	-	5.7	-	-
Graphitic shale	4	41	3.6	45	210	-	10	8.9	7.2	-	63	1.4	-	-	98	-	-
Quartzite	5	48	3.5	2.3	320	-	0.75	0.23	0.11	-	0.039	0.017	-	-	0.74	-	-
Quartzite	6	150	28	0.91	240	-	5.8	1.0	21	-	12	13	-	-	23	-	-
Diopside marble	7	83	28	1.4	190	-	2.7	2.4	43	-	27	19	-	-	110	-	-
Marble	8	57	34	3.5	210	-	5.1	5.1	78	-	73	21	-	-	290	-	-
Pyrite	9	160	17	$5.3 * 10^{-9}$	1.0	-	4600	230	$5.8 * 10^{-6}$	-	4.8	$9.1*10^8$	-	-	39	-	-
Calcite vein	10	110	260	0.32	110	-	1.5	5.1	410	-	120	380	-	-	310	-	-
Calcite	11	130	$3.6 * 10^{11}$	$3.9 * 10^{-9}$	1.2 * 10-7	-	0.67	6.4	350	-	1400	$3.6 * 10^{11}$	-	-	530	-	-
Carbonate	12	120	3700	-	-	0.075	4.1	6.3	340	81	4700	-	-	-	840	-	10
Carbonate	13	120	4800	0.33	2.3	0.084	3.5	6.1	360	75	6400	19000	-	-	840	-	11
Surface carbonate	14	160	1500	-	-	0.091	2.8	5.6	370	58	8400	-	-	-	450	-	7.7
Surface carbonate	15	240	460	0.33	8.3	0.17	2.0	12	340	20	3200	9600	-	-	740	-	38
Surface carbonate	16	190	10000	-	-	0.044	2.5	14	360	130	20000	-	-	-	1400	-	11
Water-rock interaction experiments																	
Quartzite	17	240	1.8	38	810	23	65	1.7	0.23	0.018	2.8	0.073	0.0078	3.2	0.11	20	6.0
Greenschist	18	800	61	2.7	830	5.8	40	14	52	0.28	140	36	0.036	28	25	0.83	98
Gneiss	19	1800	21	4.2	730	50	21	12	1.2	0.012	13	2.7	-	-	10	-	980
Schistose granite	20	1300	10	4.4	540	55	41	13	0.42	0.0073	4.8	1.1	0.033	-	5.6	44	970
Gabbros	21	1500	4.2	2.9	620	16	24	13	0.77	0.025	5.7	2.0	-	-	10	-	310
Carbonate rock	12	22	27	3.7	190	6.0	200	46	590	9.3	170	69	7.8	-	5700	1.7	600
Pyrite	22	28	34	1.6	110	0.18	4.0	4.0	46	6.1	20	16	0.00082	0.029	13	0.0016	2.1
Bulk Meltwater	-	440	17	1.0	780	4.9	66	6.1	31	0.45	18	18	0.003	1.3	150	0.07	360
In-situ Type-2 meltwater	-	330	23	0.34	1100	4.2	110	8.9	26	0.47	2.9	8.3	0.0046	1.6	100	0.20	230
In-situ Type-3 meltwater	-	360	19	0.43	510	1.1	110	29	54	3.1	17	40	0.0027	1.0	120	0.026	31

Inter-mineral ratios. Inter-mineral element ratios in bulk meltwaters are shown in Figure 5 and Table 6. Ratios of Sr with Rb and Al, and Ca with Na and K, all decrease with increasing discharge, which suggests the relative proportion of carbonate weathering decreases relative to K-silicate (K and Rb) and aluminosilicate (Al) weathering as discharge increases and water residence

times decrease in the subglacial environment (Figure 5a). This is in agreement with previous provenance calculations applied to the 1999 ablation season which utilizes major ions concentrations (after Sharp *et al.*, 1995a; Brown *et al.*, 1996a) (Figure 5d) and is likely to reflect a deficit between the rate of proton supply and proton consumption by carbonates at higher discharges in subglacial channels when SSCs are high (Brown *et al.*, 1994a). The slower rate of proton consumption by silicates predominately in the distributed system can be satisfied by proton availability, but more rapid rates of proton consumption by carbonates predominantly in the channellised system cannot. However, Sr / K increases with increasing discharge, and thus contradicts assertions dawn from the other inter-mineral ratios, indicating the complexity of using such inter-mineral ratios.

Indeed, ratios between species that are indicative of carbonate and silicate weathering relative to sulphide weathering are similarly hard to interpret. Sr / SO_4^{2-} and Ca / SO_4^{2-} suggests the relative proportion of carbonate weathering increases relative to sulphide weathering with increasing discharge and shorter water residence times in the subglacial environment (Figure 5). Similarly K / SO_4^{2-}, Na / SO_4^{2-}, Al / SO_4^{2-} and Al / Co increase with discharge, suggesting that the relative proportion of silicate to sulphide weathering increases with increasing discharge, as subglacial water residence time decreases (Figure 5). This further suggests sulphide oxidation is indicative of water routing through a distributed subglacial system, where sulphides are oxidised at the site of rock-flour generation in the distributed system, and sulphide oxidation provides proportionally more solute at lower discharges when water from the distributed system dominates bulk meltwaters (Brown *et al.*, 1996a). However, Sr / Co, the other inter element ratio for carbonate versus sulphide weathering, exhibits an opposite association with discharge than Sr / SO_4^{2-} and Ca / SO_4^{2-}. Similarly, Rb / Co, the other inter element ratio for silicate versus sulphide weathering exhibits an opposite association with discharge than K / SO_4^{2-}, Na / SO_4^{2-}, Al / SO_4^{2-} and Al / Co. Therefore, inter-mineral ratio data indicates the complexity of using minor and trace elements as lithogenic and hydrological tracers, and suggests dissolved ion ratios will be controlled more by physico-chemical than hydrological parameters.
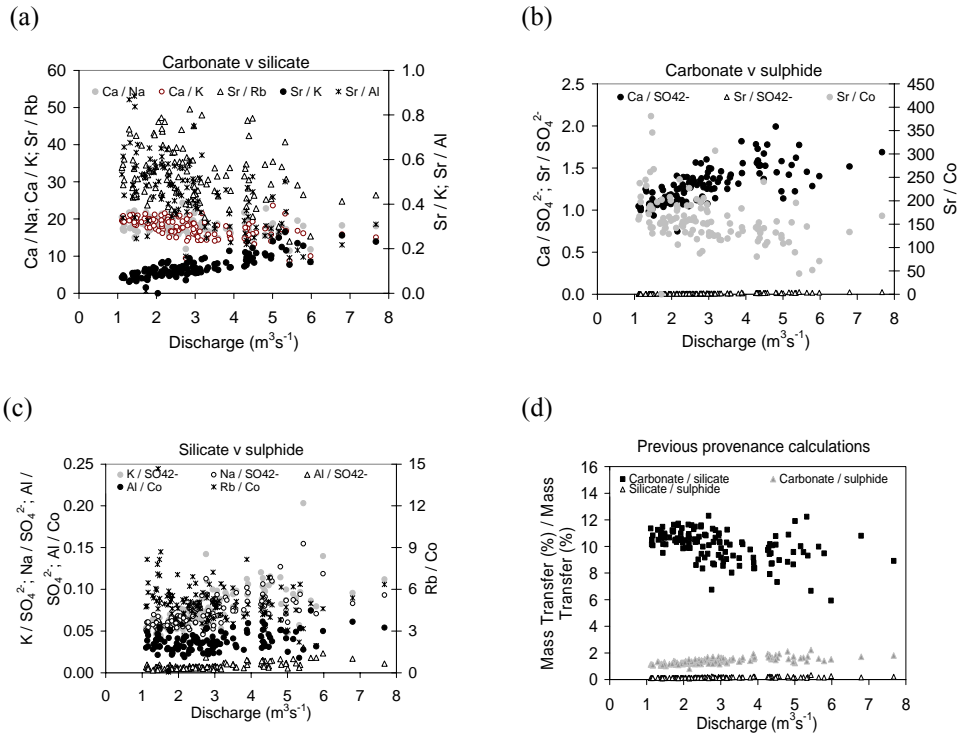
(a)

(b)

(c)

(d)

Figure 5. Inter-mineral element ratios from bulk meltwaters during the 1999 ablation period. (a) indicative of carbonate versus aluminosilicate weathering. (b) indicative of carbonate versus sulphide weathering, and (c) indicative of silicate versus sulphide weathering, and (d) from existing solute provenance calculations applied to the 1999 bulk meltwater major ion composition (after Sharp *et al*., 1995a; Brown *et al*., 1996a).

CRITIQUE AND CONCLUSIONS

While the analysis of minor and trace elements in meltwaters offers new insights into the environmental geochemistry of nival and glacierised catchments, the complex controls on the aqueous geochemistry confound simple interpretations of flow-routing in these environments. Over seasonal timescales, the dissolved concentrations of many minor and trace elements (*e.g.* Sr, Rb, Ti, Al, Co) reflect the effect of hydrological conditions such as water residence time and water-rock ratios which when used in conjunction with rock digests and water-rock interaction experiments, can reveal important information about solute sources, the nature of weathering processes, and temporal changes in weathering reactions which may be associated with hydrological conditions.

Intra-mineral ratios are a useful method for identifying dominant solute sources and the nature of weathering processes which modify the chemistry of snow- and icemelt during transit through the hydroglacial system. Utilising elements that appear to be derived from the same mineral or mineral group source, based on natural geochemical associations, rock digests and water-rock interaction experiments, can suggest the dominant lithogenic solute sources in meltwaters. For example, at HGA K / Rb and Ca / Sr ratios indicate that both silicate and carbonate weathering may be incongruent and that Sr is derived mostly from carbonate minerals. Incongruent carbonate dissolution has not been considered in previous solute provenance studies at HGA (*e.g.* Brown *et*

al., 1996a) and other glaciers (Hodson *et al*., 2000), which highlights the potential use of intra-mineral ratios for deconvoluting geochemical weathering processes operating in glacierised catchments. Additionally, Ca / Sr ratios from rock-dissolution experiments and meltwaters further suggest non-carbonate sources may supply a large but unquantifiable proportion of Ca^{2+} to bulk meltwaters. However, the equivocal provenance of many minor and trace elements, and the complex behaviour of these elements in solution (Mitchell *et al*., 2001; Mitchell, 2002), hinders the utility of intra-mineral ratios. For example, in the HGA catchment it is particularly hard to identify SO_4^{2-} sources using minor and trace element ratios since water-rock interaction experiments liberate SO_4^{2-} at very low concentrations, and elements which are liberated at high concentrations from pyrite (*e.g.* Ni and Co), are also derived in significant quantities from other minerals (*e.g.* magnetite and ferromagnesian minerals).

This also study demonstrates that inter-mineral solute ratios in meltwaters are also useful for demonstrating temporal changes in the relative proportion of carbonate, silicate and sulphide minerals weathered in the dynamic hydroglacial environment. However, field derived dissolved ion ratios are often equivocal (*e.g.* Sr / SO_4^{2-} and Sr / Co). These discrepancies between inter-mineral ratio-pairs suggest: i) species may not be derived from the hypothesized lithogenic source, ii) species may be liberated in large quantities from more than one lithogenic source, and / or iii) species concentration reflects physico-chemical controls more than hydrological controls. Nevertheless, the origin and relative concentration of minor and trace elements are likely to be similar between glacierised catchments underlain by igneous and metamorphic bedrock, reflecting common element associations in minerals, and the relative mobility in high pH glacial meltwaters.

ACKNOWLEDGEMENTS

REFERENCES

Benoit, G. and T. F. Rozan (1999). The influence of size distribution on the particle concentration effect and trace metal partitioning in rivers. *Geochimica Et Cosmochimica Acta* **63**: 113–127.

Blake, EW, and Clarke, GKC (1991). Subglacial water and sediment samplers. *Journal of Glaciology* **37**: 188–190.

Bottrell, SH and Tranter, M (2002). Sulphide oxidation under partially anoxic conditions at the bed of Haut Glacier d'Arolla, Switzerland. *Hydrological Processes* **16**: 2363–2368.

Brown, GH. 2002. Glacier meltwater hydrochemistry. *Applied Geochemistry* **17**: 855–883.

Brown, GH, Sharp, M, Tranter, M, Gurnell, AM, Nienow, PW. 1994a. Impact of post mixing chemical reactions on the major ion chemistry of bulk meltwaters draining the Haut Glacier d'Arolla, Valais, Switzerland. *Hydrological Processes* **8**: 465–480.

Brown, GH, Tranter, M, Sharp, MJ, Davis, TD, and Tsiouris, S. 1994b. Dissolved oxygen variations in Alpine glacial meltwaters. *Earth Surface Processes and Landforms* **19**: 247–253.

Brown, GH, Tranter, M, Sharp, M. 1996a. Subglacial chemical erosion—Seasonal variations in solute provenance, Haut Glacier d`Arolla, Switzerland. *Annals of Glaciology* **22**: 25–31.

Brown, GH, Sharp, M, Tranter, M. 1996b. Experimental investigations of the weathering of suspended sediment by Alpine glacial meltwater. *Hydrological Processes* **10**: 579–597.

Brown, GH, Fuge, R. 1998a. Trace element chemistry of glacial meltwaters in an Alpine headwater catchment. In *Hydrology, Water Resources and Ecology in Headwaters (Proceedings*

of the Headwater 1998 Conference held at Meran/Merano, Italy, April, 1998). International Association of Hydrological Sciences Publication **248**: 435–442.

Brown, GH, Fuge, R. 1998b. Minor and trace element chemistry and provenance in Alpine glacial meltwaters. In *Water-Rock Interaction*. Arehart and Hulston (eds). Balkema: Rotterdam; 297–300.

Brown, GH, Hubbard, B, Seagren, AG. 2001. Kinetics of solute acquisition from the dissolution of suspended sediment in subglacial channels. *Hydrological Processes* this volume.

Carroll, D. 1974. *Rock Weathering*. Chapman and Hall: London

Collins, DN. 1979. Quantitative determination of the subglacial hydrology of two Alpine glaciers. *Journal of Glaciology* **23**: 347–360.

Dal Piaz, GV, De Vecchi, Gp, Hunzicker, J 1977. The Austroalpine layered gabbros of the Matterhorn and Mont Collon-Dents de Bertol. *Schweizerische Mineralogische und Petrografische Mitteilungen* **57**: 59–81.

Deer, WA., Howie, RA, and Zussman, J. 1992. *An introduction to the rock forming minerals,* Longman.

Drever, JI, Hurcomb, DR. 1986. Neutralization of atmospheric acidity by chemical weathering in an alpine basin in the North Cascade Mountains. *Geology* **14**: 221–224.

Fairchild, IJ, Bradby, L, Sharp, M, Tison, J-L. 1994. Hydrochemistry of carbonate terrains in Alpine glacial settings. *Earth Surface Processes and Landforms* **19**: 33–54.

Fairchild, IJ., Killawee, JA, Hubbard, B and Dreybrodt W. 1999. Interactions of calcareous suspended sediment with glacial meltwater: a field test of dissolution behaviour. *Chemical Geology* **155**: 243–263.

Gordon, S, Sharp, M, Hubbard, B, Smart, C, Ketterling, B and Willis, I. 1998. Seasonal reorganization of subglacial drainage inferred from measurements in boreholes. *Hydrological Processes* **12**: 105–133.

Hodson, A, Tranter M, Vatne G. 2000. Contemporary rates of chemical denudation and atmospheric CO_2 sequestration in glacier basins: An Arctic perspective. *Earth Surface Processes and Landforms* **25**: 1447–1471.

Hubbard, BP, Sharp, MJ, Willis, IC, Nielsen, MK and Smart CC. 1995. Borehole water-level variations and the structure of the subglacial hydrological system of Haut Glacier d'Arolla, Valais, Switzerland. *Journal of Glaciology* **41**: 572–583.

Jacobson, AD, Blum JD and Walter LM. 2002. Reconciling the elemental and Sr isotope compostion of Himalayan weathering fluxes: Insignts from the carbonate geochemistry of stream waters. *Geochimica et Cosmochimica* **66**: 3417–3429.

Levinson, AA. 1980. *Introduction to Exploration Geochemistry.* Applied Publishing Ltd.: Wilmette; 924.

Mazurek, M. 1986. Structural evolution and metamorphism of the Dente Blanch nappe and the Combin zone west of Zermatt (Switzerland). *Eclogae Geologicae Helvetaie* **79**: 41–56.

Mitchell, A, Brown GH and Fuge, R. 2001. Minor and trace element export from a glacierised Alpine headwater catchment (Haut Glacier d'Arolla, Switzerland). *Hydrological Processes* **15**: 3499–3524.

Mitchell, AC., 2002. *Reaction modelling, solute provenance and aqueous geochemistry in subglacial environments.* Ph.D., University Of Wales, Aberystwyth: 333.

Nienow, P, Sharp, M, Willis, I. 1996. Velocity-discharge relationships derived from dye-tracer experiments in glacial meltwaters: implications for subglacial flow conditions. *Hydrological Processes* **10**: 1411–1426.

Poulton, SW and Raiswell, R. 2005. Chemical and physical characteristics of iron oxides in riverine and glacial meltwater sediments. *Chemical Geology* **218**: 203–221.

Raiswell, R. 1984. Chemical models of solute acquisition in glacial melt waters. *Journal of Glaciology* **30**: 49–57.

Reinmann, D, Caritat, P. 1998. *Chemical elements in the environment. Fact sheets for the geochemist and environmental scientist.* Springer: Berlin; 397.

Seagren, AG. 1999. *The Nature of Solute Acquisition and Suspended Sediment Dynamics in Channellised Subglacial Weathering Environments, Haut Glacier d'Arolla, Valais, Switzerland.* Ph.D., University Of Wales, Aberystwyth**:** 306.

Sharp, M. 1991. Hydrological inferences from meltwater quality data: the unfulfilled potential. *Proceedings of the British Hydrological Society (BHS) 3rd National Hydrological Symposium, Southampton*, 5.1–5.8.

Sharp, M, Richards, KS, Willis, I, Arnold, N, Nienow, P, Lawson, W, Tison, JL. 1993. Geometry, bed topography and drainage system structure of the Haut Glacier d'Arolla. Switzerland, *Earth Surface Processes and Landforms* **18**: 557–571.

Sharp, M, Tranter, M, Brown, GH, Skidmore, M. 1995a. Rates of chemical denudation and CO_2 drawdown in a glacier-covered alpine catchment. *Geology* **23**: 61–64.

Sharp, M, Brown, GH, Tranter, M, Willis, I, Hubbard, B. 1995b. Comments on the use of chemically based mixing models in glacier hydrology. *Journal of Glaciology* **41**: 241–246.

Stumm, W, Morgan, JJ. 1996. *Aquatic chemistry: chemical equilibria and rates in natural waters (3rd edition).* Wiley: New York; 1040.

Tranter, M, Brown, GH, Raiswell, R, Sharp, M, Gurnell, A. 1993. A conceptual model of solute aqusistion by Alpine glacial meltwaters. *Journal of Glaciology* **39**: 573–581.

Tranter, M, Sharp, M, Brown, GH, Willis, IC, Hubbard, BP, Nielsen, MK, Smart, CC, Gordon, S, Tulley, M, Lamb, H. 1997. Variability in the chemical composition of in situ subglacial meltwaters. *Hydrological Processes* **11**: 59–77.

Tranter , M. and H. G. Jones. 2000. The Chemistry of Snow: Processes and Nutrient Cycling. H. G. Jones, J. Pomeroy, D. A. Walker and R. Wharton. *Snow Ecology.* Cambridege, Cambridge University Press. 127–167.

Tranter, M, Sharp, MJ, Lamb, HR, Brown, GH, Hubbard, BP and Willis IC. 2002. Geochemical weathering at the bed of Haut Glacier d'Arolla, Switzerland—A new model. *Hydrological Processes* **16**: 959–993.

White, AF, Schulz, MS, Lowenstern, JB, Vivit, DV and Bullen, TD. 2005. The ubiquitous nature of accessory calcite in granitoid rocks: Implications for weathering, solute evolution, and petrogenesis. *Geochimica et Cosmochimica Acta* **69**: 1455–1471.